JOURNAL OF AGRICULTURAL AND FOOD CHEMISTRY

pubs.acs.org/JAFC

Article

A Genomics-Based Semirational Approach for Expanding the Postbiotic Potential of Collagen Peptides Using Lactobacillaceae

Ji-Young Lee,[¶] Hye Won Hwang,[¶] Hyeon-Su Jin, Jae-Eun Lee, Nam Joo Kang, and Dong-Woo Lee*

Cite This: *J. Agric. Food Chem.* 2022, 70, 8365−8376

Read Online

ACCESS | Metrics & More | Article Recommendations | Supporting Information

ABSTRACT: Food-derived bioactive peptides (BPs) have received considerable attention as postbiotics for human gut health. Here we used a genomics-based semirational approach to expand the postbiotic potential of collagen peptides (CPs) produced from probiotic fermentation. *In silico* digestion revealed distinct BPs embedded in fish collagen in a protease-dependent manner. Anaerobic digestion of collagen by representative Lactobacillaceae species revealed differential substrate utilization and collagen degradation patterns. Nanoliquid chromatography−mass spectrometry analysis of CPs showed that each species exhibited different cleavage patterns and unique peptide profiles. Remarkably, the 1−10 kDa CPs produced by *Lacticaseibacillus paracasei* showed agonistic activities toward G protein-coupled receptor 35 (GPR35). These CPs could repair intestinal epithelium through the GPR35-mediated extracellular signal-regulated protein kinase (ERK) 1/2 signaling pathway, suggesting that probiotic-aided collagen hydrolysates can serve as postbiotics for host−microbe interactions. Therefore, this study provides an effective strategy for the rapid screening of CPs for gut health in the gastrointestinal tract.

KEYWORDS: *collagen peptides, postbiotics, bioactive peptides, gut, Lactobacillaceae*

INTRODUCTION

Bioactive peptides (BPs) play a crucial role in human physiology and metabolism, as biological mediators such as hormones, neurotransmitters, and antimicrobial agents.[1] There is an increase in the number of peptide drugs in the global market that target metabolic disorders by modulating extracellular signaling receptors.[2] Recently, peptide therapeutics have diversified beyond disease treatment to provide nutritional benefits and health-promoting properties as nutraceuticals.[3,4] BPs derived from food by means of enzymatic hydrolysis or microbial fermentation show various physiological benefits, including antihypertensive, antioxidant, antimicrobial, and antiobesity effects.[1,5,6]

Fish and marine organisms have been recognized as rich sources of bioactive compounds with valuable nutraceutical and medical food potentials.[7] The classical food application of gelatin is mainly based on its gel-forming properties in emulsifiers, foaming agents, and colloidal stabilizers. Besides its gel-forming nature, fish collagen is a promising protein source for modulating human physiology and metabolism, with enhanced physicochemical properties, biocompatibility, and stability.[8] In this regard, the enzymatic hydrolysis of collagen or gelatin for the production of BPs has received attention in the past decade. Collagen peptides (CPs) provide not only various health benefits (e.g., such as protection against skin aging, acceleration of wound healing, promotion of bone health, improvement in muscle strength, and prevention of obesity) but also excellent absorption and metabolism in animal models and human studies.[9−12]

Recent studies have highlighted the impact of the host diet on the composition of the gut microbiota and their metabolites.[13] Microbial metabolites, including peptides, play a crucial role in physiological functions such as immune responses, metabolism, neurotransmission, and reproduction. For instance, bacterial short-chain fatty acids (SCFAs) such as butyrate contribute to O_2 consumption and barrier function in the host epithelium.[14] Indole-derivatives regulate the gut immune system to brain signaling.[15] In addition, di- and tripeptides derived from soy alleviate gut inflammation in the dextran sulfate sodium-induced pig model.[16] These molecules diffuse into cells or bind to specific receptors such as G protein-coupled receptors (GPCRs) as metabolite sensors to activate cell-signaling pathways.[17] In contrast, dysbiosis of gut microbiota harms the host immune system and gut metabolic homeostasis, leading to diabetes, obesity, inflammatory bowel disease (IBD), autoimmune diseases, and cancers.[18]

In the human gut, food-fermenting lactic acid bacteria (LAB) possess a complex proteolytic system because of their amino acid auxotrophy.[19] In this regard, Lactobacillaceae can serve as biocatalysts to produce food-derived BPs that are beneficial for host physiology and gut homeostasis. However, in the same Lactobacillaceae family, individual species possess distinct proteins, implying that they have differential protease repertoires to produce food-derived peptide portfolios.[20,21] In the present study, we designed and developed a genomics-aided semirational approach using Lactobacillaceae fermentation to

Received: February 18, 2022
Revised: June 7, 2022
Accepted: June 7, 2022
Published: June 27, 2022

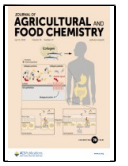

investigate the potential impact of collagen BPs as postbiotics for human gut health.

MATERIALS AND METHODS

Fish Gelatin. Fish gelatin (Vinh Wellness, Vietnam) was obtained from Newtree Co., Ltd. (Republic of Korea). We used gelatin as a substrate for anaerobic digestion by Lactobacillaceae species to produce collagen peptides. Refer to Bacterial Strains and Culture Conditions and Preparation of Collagen Hydrolysates and Peptide Fractions for detailed processes.

Bacterial Strains and Culture Conditions. *Lactobacillus* strains were obtained from the Korean Culture Center of Microorganisms (KCCM), South Korea (Table S1). Bacterial cells were precultured in sealed anaerobic serum bottles containing *Lactobacilli* de Man, Rogosa, and Sharpe (MRS) broth (Difco, Detroit, MI) at 37 °C under a gas mixture of 10% CO_2, 10% H_2, and 80% N_2. Precultured cells at the late exponential phase (2.0×10^7 cells/mL) were transferred to anaerobically prepared defined media (DM) and incubated at 37 °C for 48 h (Table S2).[22]

Briefly, *Lactiplantibacillus plantarum* Korean Collection for Type Culture (KCTC) 3108, *Lacticaseibacillus rhamnosus* KCTC 3237, *Lacticaseibacillus paracasei* KCTC 3510, *Lacticaseibacillus casei* KCTC 3109, and *Limosilactobacillus fermentum* KCTC 3112 were grown in DM. *Ligilactobacillus salivarius* KCCM 40998 was cultured in DM supplemented with 2× amino acid concentration (DM2). *Limosilactobacillus reuteri* KCCM 40717 and *Lactobacillus delbrueckii* KCTC 3635 were grown in DM supplemented with 0.1% and 0.5% yeast extract, respectively (DM3 and DM4, respectively). *Lactobacillus acidophilus* KCCM 32820 and *Lactobacillus gasseri* KCTC 3163 were cultured in 1/5× MRS. Lactobacillaceae species were cultivated in appropriate DM supplemented with 0.5% fish collagen (DMC) for growth kinetics and substrate utilization experiments.

Bacterial growth was monitored by measuring the optical density at 600 nm (OD_{600}) using a spectrophotometer (Libra S70; Biochrom, Cambridge, U.K.). For direct cell counting, a Neubauer chamber was used (depth, 0.1 mm; area, 0.0025 mm^2; Paul Marienfeld GmbH & Co. KG, LaudaKönigshofen, Germany) with a phase-contrast microscope (BX43; Olympus, Tokyo, Japan).

Preparation of Collagen Hydrolysates and Peptide Fractions. After 48 h of incubation, cells were harvested by centrifugation (8 000*g* for 20 min at 4 °C) and stored at −80 °C until further use. The cell-free supernatant was 20-fold concentrated at 70 °C for >20 h and centrifuged at 10 000*g* for 1 h at 4 °C to remove the precipitate. The resulting supernatant was filtered through a 0.2 μm pore-size membrane (Millipore, Bedford, MA). The filtrate was then fractionated through stepwise ultrafiltration using a 10 kDa cutoff disc (Millipore) membrane to obtain high molecular weight (HMW, >10 kDa) and low molecular weight (LMW, <10 kDa) fractions. For size-exclusion chromatography, samples were loaded at a rate of 1.5 mL/min onto a Superdex 30 prep grade (pg) column (90 mL) pre-equilibrated with 20 mM Tris-HCl (pH 7.0) in a Biologic DuoFlow FPLC System (Bio-Rad, Hercules, CA). Eluents were monitored by measuring the absorbance at 210 nm, following which each peak fraction was pooled, lyophilized, and stored at 4 °C until use. Based on the standard curve using proteins/peptides of known sizes, 1−10 kDa peptide fractions were pooled and used for further analysis.

GPCR β-Arrestin Assay. The screening assay was conducted using the gpcrMax panel at Eurofins Profiling Services (Eurofins DiscoverX, Fremont, CA). The 1−10 kDa peptide fractions (1 mg/mL) were screened in a cell-based assay of 168 GPCRs using β-arrestin recruitment. The samples were tested for their agonistic activation of GPCRs in cells derived from Chinese hamster ovary-K1, U2OS, and human embryonic kidney 293. Briefly, cells were seeded and incubated at 37 °C prior to testing. Cells were then incubated with samples or appropriate agonists to induce responses. Signals were generated by adding the PathHunter Detection reagent cocktail. Data were expressed as a percentage of control ligands. All experiments were performed in duplicate.

Peptide Identification Using Liquid Chromatography with Tandem Mass Spectrometry (LC-MS/MS). For LC-MS/MS analysis of collagen hydrolysates, peptides were analyzed using reversed-phase high-performance liquid chromatography/electrospray ionization tandem mass spectrometry with a Nano LC-2D Ultra system (Eksigent, Dublin, CA) coupled to a nanoelectrospray LTQ XL linear ion trap mass spectrometer (Thermo Fisher Scientific, Waltham, MA). Peptides (3 μg) were loaded onto a trap column [internal diameter (ID) = 75 μm; New Objective IntegraFrit, Scientific Instrument Services Inc., Ringoes, NJ] and eluted onto an analytical column [ID = 75 μm, outside diameter (OD) = 375 μm; Molex Polymicro Technologies, Phoenix, AZ] at a flow rate of 0.4 μL/min. Both columns were packed in-house with ReproSil-Pur 200 C18-AQ 5 μm particles (Dr. Maisch GmbH, Ammerbuch, Germany). The mobile phase consisted of 0.1% (v/v) formic acid (FA) in water (solvent A) and 0.1% (v/v) FA in acetonitrile (ACN) (solvent B). The gradient parameters were 0−1 min (2%−5% solvent B), 1−62 min (5%−35% solvent B), 62−65 min (35%−60% solvent B), 65−67 min (60% solvent B), 67−70 min (60%−2% solvent B), and 70−90 min (2% solvent B), with a total run time of 90 min (or a 60 min with steeper gradient). MS analysis of peptide eluents was performed on an LTQ XL linear ion trap mass spectrometer (Thermo Fisher Scientific) in positive-ion mode with a nano ion spray voltage of 1.8 kV and an interface heater temperature of 200 °C. The normalized collision energy was set to 35% for MS/MS analysis.

For peptide identification, 1−10 kDa peptide fractions were analyzed using an UltiMate 3000 RSLC nano system (retention time RSD <0.2%) coupled to a Q-Exactive Orbitrap HF-X mass spectrometer (Thermo Fisher Scientific). Peptides (2 μg) were loaded onto a trap column (ID = 75 μm × 2 cm, packed with Acclaim PepMap 100 C18, 3 μm, 100 Å; Thermo Fisher Scientific) and eluted onto an analytical column (ID = 75 μm × 50 cm, packed with PepMap RSLC C18, 2 μm, 100 Å; Thermo Fisher Scientific) at a flow rate of 0.27 μL/min. Mobile phase A for LC separation was 0.1% FA in deionized water, while mobile phase B was 0.1% FA in ACN. The chromatography gradient was set up to give a linear increase from 5% B to 10% B over 5 min, from 10% B to 35% B over 65 min, 35% B to 50% B over 10 min, 50% B to 80% B over 5 min, 80% B to 80% B over 5 min, and 80% B to 5% B over 5 min. For tandem mass spectrometry, mass spectra were acquired using data-dependent acquisition with a full mass scan (400−2000 m/z), followed by MS/MS scans. The spray voltage was 1.8 kV, and the heated capillary temperature was 250 °C. The normalized collision energy was set to 27% for MS/MS analysis.

Data Analysis. For data analysis, the integrated tools in PeptideShaker were used. First, the MS spectra were processed using a ThermoRawFileParser to convert raw data into peak lists (.mzML format). Processed spectra were compared using the target decoy database search strategy with the FASTA database of *Pangasianodon hypophthalmus* (striped catfish) (UniProt proteome identifier UP000327468) and *L. paracasei* JCM 8130 [National Center for Biotechnology Information (NCBI) GenBank assembly accession GCA_000829035.1], *L. plantarum* DSM 20174 (GCA_014131735.1), or *L. salivarius* BCRC 12574 (GCA_002735985.1). For the MS-GF+ search, oxidation (+15.99) of methionine and proline were set as variable modifications. The precursor m/z tolerance was ±10.0 ppm and ±2.0 Da, and the fragment m/z tolerance was ±20.0 ppm and ±0.5 Da, for Q-Exactive Orbitrap and LTQ-XL, respectively. A list of proteins and peptides was obtained, with a false discovery rate of less than 0.01 (1%).

The physicochemical properties of peptides were identified from MS spectral data (mass) or predicted using *in silico* tools [IPC 2.0, to predict isoelectric points (p*I*)] (http://ipc2.mimuw.edu.pl/). To analyze peptide bioactivities, previously characterized sequences regulating mucosal activity or showing antioxidative and anti-inflammatory activities were retrieved from the BIOPEP database. The sequence logo representation of collagen cleavage sites was visualized by implementing the ggseqlogo package in R, which is freely available at the Github repository.

Bioinformatics Tools. *In silico* proteolysis of collagen was performed by implementing a cleaver package in R, which is freely

https://doi.org/10.1021/acs.jafc.2c01251
J. Agric. Food Chem. 2022, 70, 8365−8376

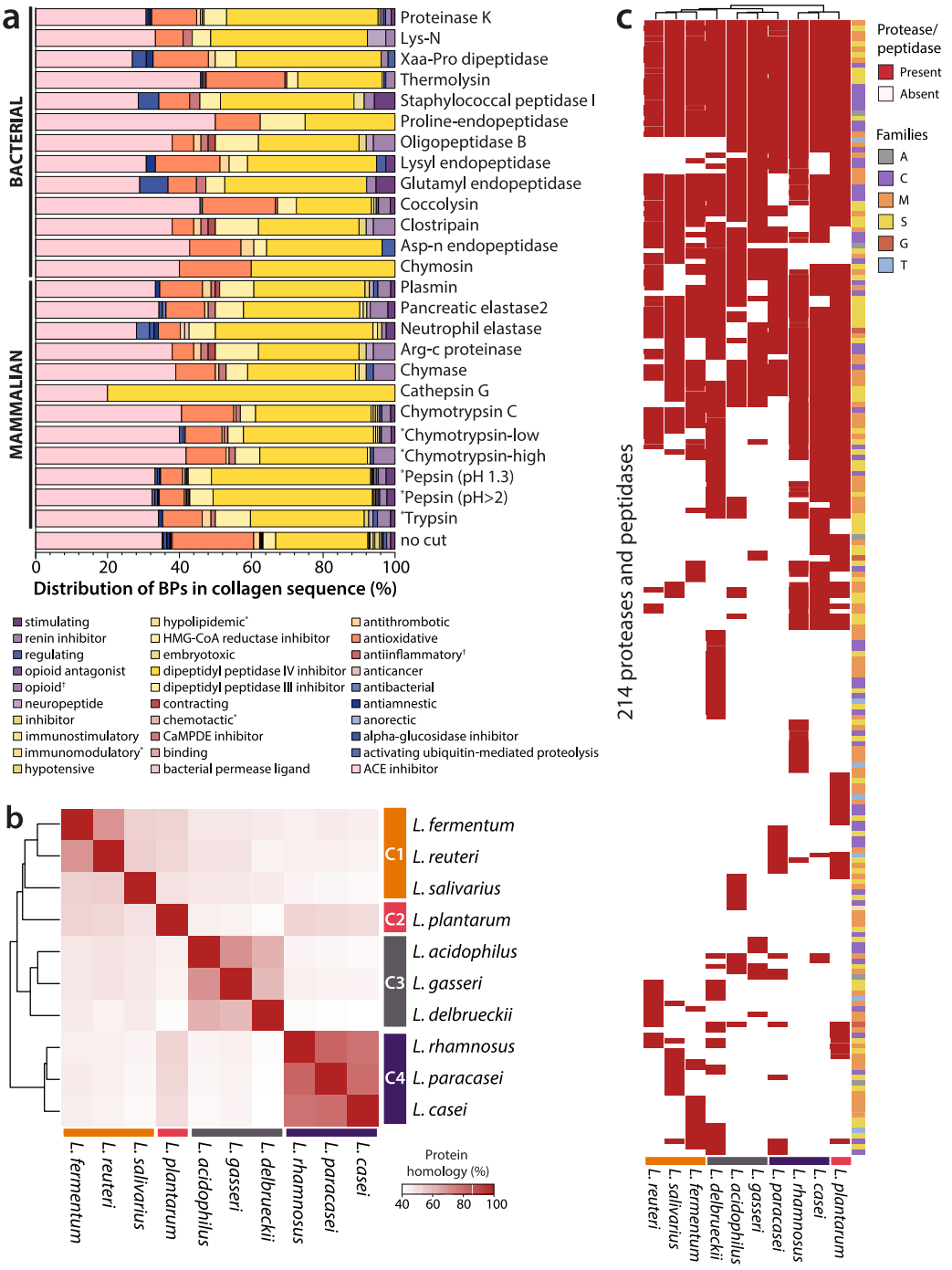

Figure 1. *In silico* analysis of collagen bioactivities and proteolytic enzymes of lactic acid bacteria. (a) Distribution of collagen-derived bioactive peptides (BPs) released through *in silico* protein digestion by 25 mammalian and bacterial proteases. *, human gastrointestinal enzymes; †, bioactivities specific to bacterial enzymes; ‡, bioactivities specific to mammalian enzymes. (b) Hierarchical clustering analysis of the percentage of conserved proteins (POCP) among 10 Lactobacillaceae species. POCP between two genomes was calculated with default parameters (*e*-value = $1 \times e^{-5}$, sequence identity = 0.4, alignment length = 0.5). See Table S1 for genome information. CX (X = 1, 2, 3, or 4) represent clusters of Lactobacillaceae species with protein similarities above 49%. Cluster 1 (C1), *L. casei* ATCC 393, *L. paracasei* JCM 8130, and *L. rhamnosus* DSM 20021; C2, *L. acidophilus* DSM 20079, *L. gasseri* ATCC 33323, and *L. delbrueckii* ATCC 11842; C3, *L. plantarum* DSM 20174; C4, *L. fermentum* B1 28, *L. reuteri* DSM 20016, and *L. salivarius* BCRC 12574. (c) Hierarchical clustering analysis of proteolytic enzymes in 10 Lactobacillaceae species. Clustering was performed and visualized using default parameters of R package ggplot::heatmap.2. Proteases and peptidases were labeled according to their families: aspartic proteases (A, gray), cysteine proteases (C, purple), glutamic proteases (G, red), metalloproteases (M, orange), serine proteases (S, yellow), and threonine proteases (T, light blue). BP, bioactive peptide.

available on the Bioconductor Web site (https://bioconductor.org/). The amino acid sequences of collagen were retrieved from the NCBI database (https://www.ncbi.nlm.nih.gov/) using the following keywords: *P. hypophthalmus* [organism] and collagen. The BIOPEP database (https://biochemia.uwm.edu.pl/biopep-uwm/) was used as a BP database to assign functions to peptide sequences.

Conserved proteins between a pair of genomes were calculated using the percentage of conserved proteins (POCP) software downloaded

https://doi.org/10.1021/acs.jafc.2c01251
J. Agric. Food Chem. 2022, 70, 8365−8376

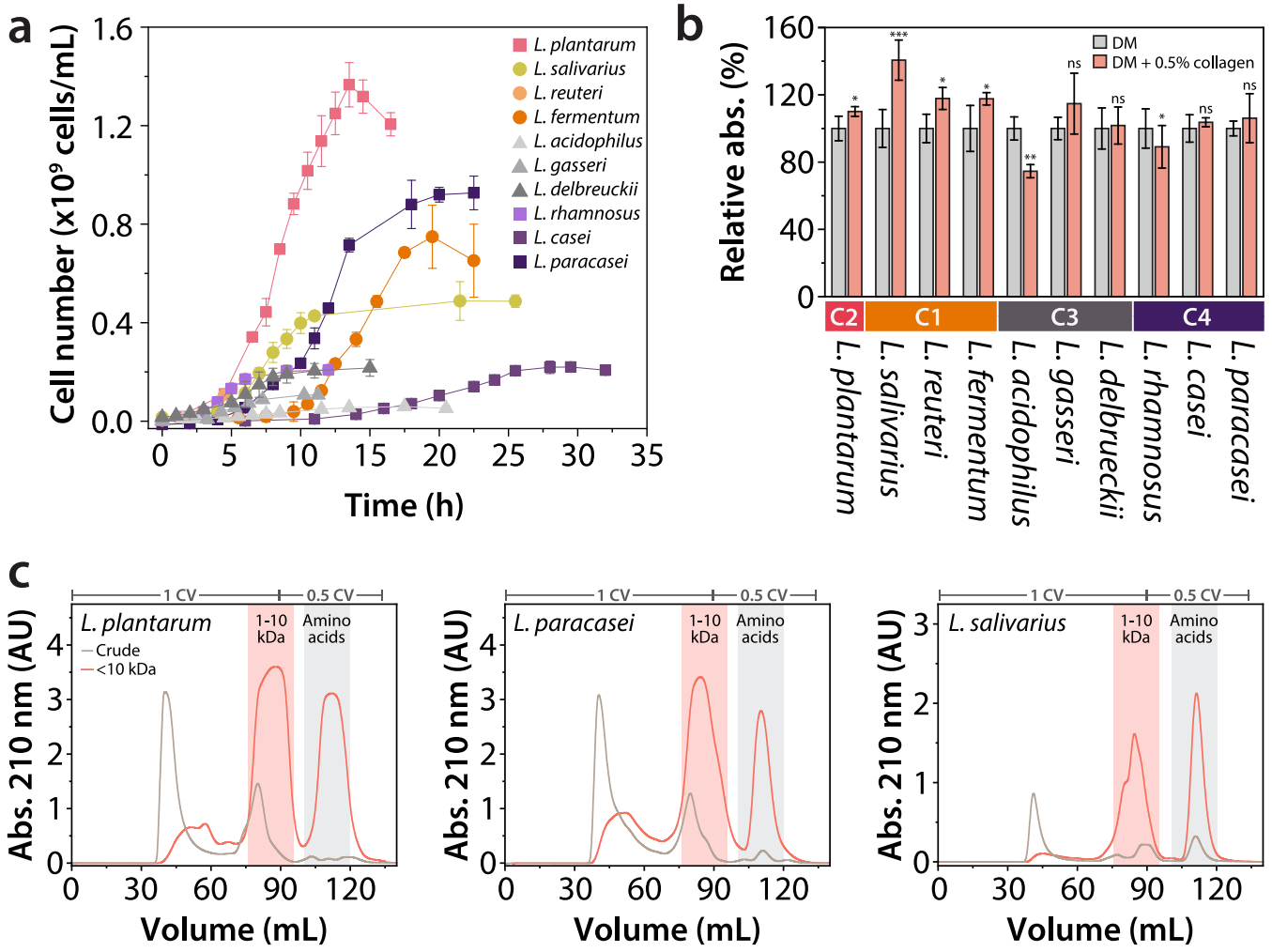

Figure 2. Growth phenotypic characterization of Lactobacillaceae species grown on collagen. (a) Growth curves of Lactobacillaceae species grown anaerobically in defined media (DM) at 37 °C (see Materials and Methods for media compositions and growth conditions). Values are represented as mean ± SD ($n = 3$). (b) Effect of collagen on the maximal cell yield of Lactobacillaceae. Values are represented as mean relative absorbance ± SD ($n = 3-14$). Statistical differences were examined using an unpaired student's *t*-test (***, $p \leq 0.001$; **, $p \leq 0.01$; *, $p \leq 0.05$; ns, $p > 0.05$). (c) Size-exclusion chromatogram of crude and low molecular weight (LMW; <10 kDa) collagen hydrolysates produced by Lactobacillaceae. Culture supernatants (*L. plantarum* LMW, 400 mg; *L. plantarum* crude, 50 mg; *L. paracasei* LMW, 200 mg; *L. paracasei* crude, 50 mg; *L. salivarius* LMW, 50 mg; *L. salivarius* crude, 4.8 mg) were loaded onto a Superdex 30 pg column (90 mL) equilibrated with 20 mM Tris-HCl buffer (pH 7.0). Chromatographic peaks were monitored at 210 nm to analyze the peptides. Gray regions represent the amino acids based on the standard curve. CV, column volume; DM, defined media.

from the GitHub repository (https://github.com/hoelzer/pocp.git) and implemented in the R module. Based on a 50% similarity cutoff limit between each pair of genomes, default parameters were used for the analyses (*e*-value = $1 \times e^{-5}$, sequence identity = 0.4, alignment length = 0.5). POCP analytical data were visualized using heatmaps generated with ggplot::heatmap.2 packages of R.

A list of proteolytic enzymes for each Lactobacillaceae species was obtained from the MEROPS database (https://www.ebi.ac.uk/merops/). Clustering of Lactobacillaceae on the basis of their proteolytic enzymes was performed and visualized using the ggplot::heatmap.2 packages of R.

Cell Culture and MTT Assay. Caco-2 cells, a human epithelial colorectal adenocarcinoma cell line, were obtained from the American Type Culture Collection (ATCC, Manassas, VA). Caco-2 cells were cultured at 37 °C in a humidified atmosphere with 5% CO_2 in Eagle's Minimum Essential Medium (EMEM) supplemented with 20% fetal bovine serum and penicillin/streptomycin.

To assess cell viability, Caco-2 cells (1×10^4 cells/well) were cultured in 96-well plates for 24 h. Cells were incubated with *L. plantarum* or *L. paracasei* CP fractions or equal fractions of DMC at final concentrations of 0, 0.01, 0.1, 1 or 10 mg/mL. After 48 h, 20 μL of 5 mg/mL thiazolyl blue tetrazolium bromide (MTT) was added per well and incubated for 2 h. Following that, the culture medium was removed, and 200 μL of dimethyl sulfoxide was added to dissolve MTT formazan crystals for 30 min. Absorbance was measured at 570 nm using a microplate reader (Sunrise-Basic Tecan, Grodig, Austria).

Wound Healing Assay. Caco-2 cells were seeded into 6-well plates, at a density of 7.5×10^5 cells/well, and cultured until 80% confluence. Cells were preincubated with the vehicle, 0.1 μM CID 2745687 (Tocris Bioscience, Bristol, U.K.) or 10 μM PD98059 (Cell Signaling Technology, Danvers, MA) for 1 h in serum-free EMEM. CID 2745687 and PD98059 were used to selectively inhibit GPR35 and mitogen-activated protein kinase kinase (MEK1/2) involved in the ERK1/2 signaling pathway, respectively. Subsequently, the cells were scratched using a sterile 200 μL tip to create wounds on the cell monolayer. The detached cells were washed with phosphate-buffered saline and then incubated in a serum-free medium containing 20 μg/mL CP fractions, 20 ng/mL human epidermal growth factor (EGF; Sigma-Aldrich, St. Louis, MO), or 2 μM zaprinast (Tocris Bioscience) for 48 h. Photographs of the wound were monitored with a microscope from 0 h, at intervals of 24 h. The width of the wound was quantified using Images Plus 3.0 ML software (Motic, Vancouver, Canada), and the relative

https://doi.org/10.1021/acs.jafc.2c01251
J. Agric. Food Chem. 2022, 70, 8365−8376

wound closure rate was calculated as the relative difference in wound width and expressed as percentage of control.

Western Blot Analysis. Caco-2 cells (1×10^6 cells/well) were cultured in a 60 mm dish for 24 h and then starved in a serum-free medium for 12 h. For the inhibitor treatment group, cells were preincubated with 0.1 μM CID 2745687 for 1 h and then treated with a vehicle, 20 μg/mL CP fractions, or specific agonists (20 ng/mL EGF or 2 μM zaprinast). After a 5 min incubation, the cells were harvested using cell lysis buffer (Cell Signaling Technology), according to the manufacturer's instructions. The protein concentration of each cell lysate was determined using the Bio-Rad Protein Assay Kit (Bio-Rad), according to the manufacturer's instructions. Cell lysates (30 μg) were separated using 10% sodium dodecyl sulfate-polyacrylamide gel electrophoresis (SDS-PAGE) and transferred to a polyvinylidene fluoride membrane (Millipore). The membrane was blocked using 5% skim milk for 3 h and incubated with the primary antibody, overnight at 4 °C. Subsequently, the membrane was incubated with a horseradish peroxidase-conjugated secondary antibody for 2 h at room temperature. The proteins were detected using an ECL Plus Western Blotting Detection System (GE Healthcare Life Sciences, Waukesha, WI). β-Actin was used as the loading control. Expression levels were quantified using ImageJ software (National Institutes of Health, Bethesda, MD).

RESULTS

***In Silico* Analysis of Collagen Bioactivities.** To identify the potential BPs embedded in collagen, 238 collagen-encoding genes were retrieved from the genome of *P. hypophthalmus* (NCBI accession number GCA_009078355.1). The deduced amino acid sequences of these genes contained 1157 sequences that could serve as putative BPs, based on a BP sequence search using the BIOPEP database. Collagen-encoding genes were digested *in silico* with proteases of which the P1-sites were characterized using Expasy Peptide Cutter (https://web.expasy.org/peptidecutter/). Consequently, 25 mammalian, bacterial, and fungal collagenolytic proteases released 768 distinct BPs in 30 different functional categories, ranging from angiotensin-converting-enzyme, inhibitory to embryotoxic peptides (Figure 1a). Notably, bacterial and mammalian proteases exhibited distinct bioactivities. For example, bacterial proteases exclusively release anti-inflammatory peptides during collagen digestion. In contrast, immunomodulatory peptides are produced upon cleavage by human digestive enzymes such as trypsin, chymotrypsin, and pepsin. These results indicated that bacterial proteases produce specific BPs that human GI enzymes cannot produce and *vice versa*. Taken together, *in silico* protein digestion revealed that bacterial proteases and/or collagen-degrading microbes might produce different peptide profiles that are not made by human GI enzymes.

Genome-Wide Analysis of Lactobacillaceae Species as Biocatalysts. To investigate whether probiotics could serve as biocatalysts for collagen degradation, 10 Lactobacillaceae-type strains approved by the Ministry of Food and Drug Safety, Korea, were selected as probiotics. Their genome sequences were obtained from the NCBI GenBank database (Table S1) and compared using the pairwise POCP analysis. The genome-based hierarchical clusters generated using POCP analysis clearly showed that the members of the Lactobacillaceae family were divided into four distinct groups, named clusters 1, 2, 3, and 4 (Figure 1b). Moreover, the proteolytic systems of Lactobacillaceae species were compared based on the MEROPS DB-based classification of proteolytic enzymes. The protease repertoire of individual Lactobacillaceae species was divided into three clusters, distinct from the results in POCP analysis (Figure 1c). However, proteases at the family level showed similar patterns to the clusters from the POCP analysis. Species in cluster 1 specifically lacked many metalloproteases (M) and cysteine proteases (C), while those in clusters 2 and 4 possessed a group of unique serine proteases (S) and metalloproteases (M) (Figure S1). This result suggests that individual proteases and/or peptidases may vary among species, but they are likely to exert similar catalytic activities when analyzed at the family levels. The consistency of the protease (peptidase) profiles with the POCP patterns of Lactobacillaceae species suggested that these bacteria could possess differential proteolytic patterns for collagen, presumably due to different proteolytic repertoires among them.

Anaerobic Fermentation of Lactobacillaceae Species with Collagen. We used appropriate DM under anaerobic conditions to investigate the anaerobic growth of Lactobacillaceae species. *L. plantarum*, *L. paracasei*, *L. fermentum*, and *L. salivarius* showed the highest cell yield (>5×10^8 cells/mL) under anaerobic conditions (Figure 2a). However, *L. acidophilus* and *L. gasseri* exhibited poor growth in DM containing 20 amino acids. Such differential growth profiles suggest that Lactobacillaceae species might have different auxotrophy for amino acids under anaerobic conditions. To further investigate the growth-enhancing effect of collagen, bacterial cells were grown for 48 h in DM supplemented with and without 0.5% (w/v) collagen, and their maximal cell yields were compared (Figure 2b). Collagen supplementation resulted in a pronounced increase in total cell yield in clusters 1 (*L. salivarius*, *L. reuteri*, and *L. fermentum*) and 2 (*L. plantarum*). In contrast, decreased or nonsignificant changes in cell yield were observed in clusters 3 (*L. acidophilus*, *L. gasseri*, and *L. delbrueckii*) and 4 (*L. rhamnosus*, *L. casei*, and *L. paracasei*). These results confirmed that Lactobacillaceae species possess different substrate preferences for proteins as nutrients.

For a detailed analysis of growth phenotypes associated with BP production, we chose *L. salivarius* (C1), *L. plantarum* (C2), *L. delbrueckii* (C3), and *L. paracasei* (C4) as BP producers representing each cluster. All four species used glucose as the primary substrate, mostly in a growth-associated manner, to support bacterial growth, regardless of the presence of collagen (Figure S2). However, their protein utilization patterns differed from one another. *L. paracasei* showed the most significant decrease in protein concentration, whereas *L. delbrueckii* and *L. salivarius* showed marginal differences in protein and amino acid concentrations. *L. plantarum* showed increased protein concentration over time. Such differential protein utilization patterns were reflected by the hydrolysis patterns of collagen in the SDS-PAGE analysis (Figure S3). *L. plantarum*, *L. salivarius*, and *L. paracasei* produced a wide range of collagen hydrolysates, whereas *L. delbrueckii* displayed only a marginal difference. However, supplementation with collagen did not cause noticeable changes in the expression of cytosolic proteins (Figure S3). Together with growth profiles, the differential substrate utilization patterns and collagen hydrolysis suggested that *Lactobacillus* species have different collagen preferences, thereby producing a variety of distinct CPs.

LC-MS/MS Analysis of CP Profiles in Lactobacillaceae Species. To examine whether differential collagen hydrolysis and substrate utilization patterns yield distinct peptide profiles, we performed LC-MS/MS analysis-aided peptide identification (Figure S4, Tables S3−S5). In the case of *L. delbrueckii*, we omitted this strain for further analyses because it showed little collagenolytic activity. The culture supernatants of *L. paracasei*, *L. plantarum*, and *L. salivarius* were fractionated into HMW

https://doi.org/10.1021/acs.jafc.2c01251
J. Agric. Food Chem. 2022, 70, 8365−8376

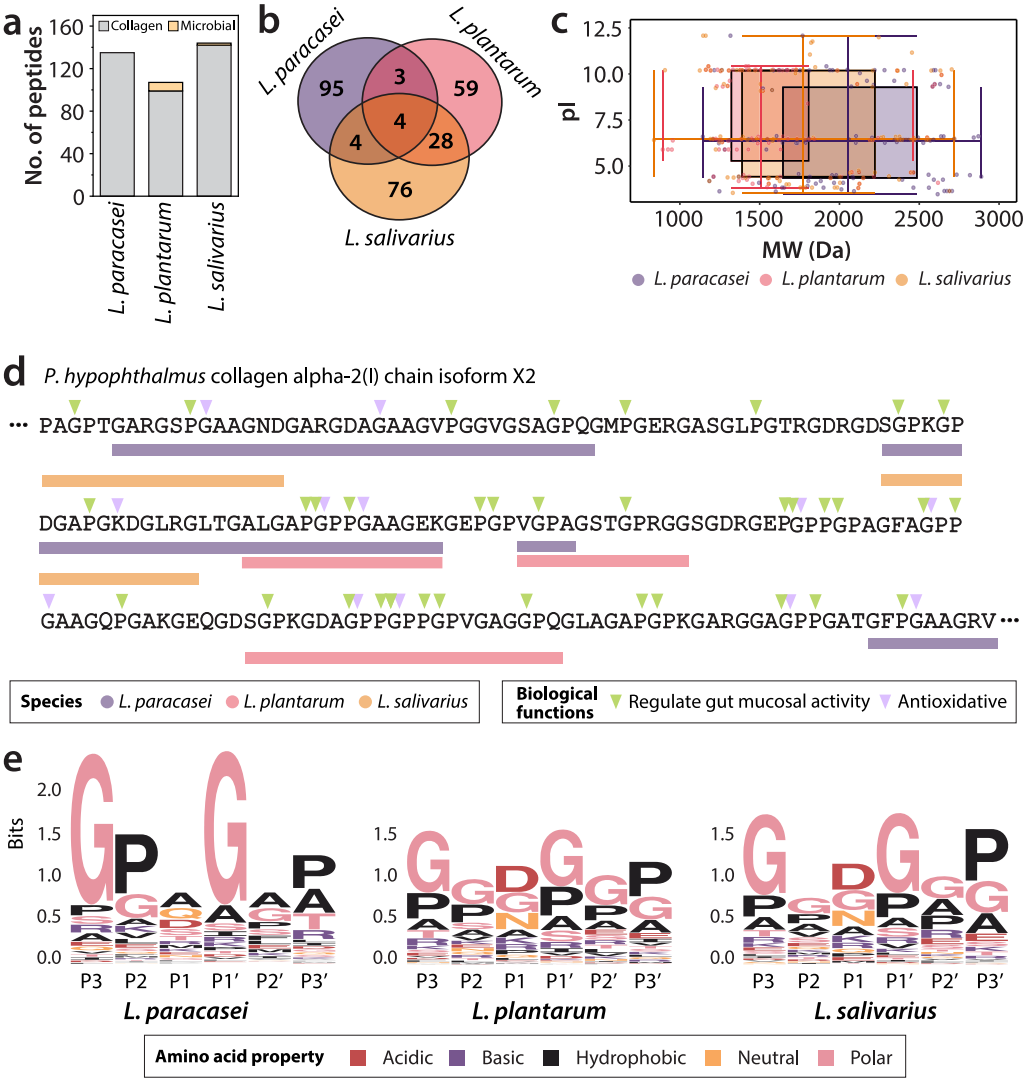

Figure 3. Mass spectrometric analysis of peptide profiles produced by Lactobacillaceae species. (a) Sources (microbial or collagen) of the peptides identified in collagen hydrolysates produced by *L. paracasei*, *L. plantarum*, and *L. salivarius*. For the protein database, *L. paracasei* JCM 8130 (GenBank accession GCA_000829035.1), *L. plantarum* DSM 20174 (GCA_ 014131735.1), *L. salivarius* BCRC 12574 (GCA_002735985.1), and *P. hypophthalmus* (UniProt ID UP000327468) were used. (b) Number of peptides identified in collagen hydrolysates produced by the three Lactobacillaceae species. (c) Distribution of molecular weights (MW) and isoelectric points (p*I*) of the identified peptides in the three Lactobacillaceae species. (d) Differential distribution of peptides on a representative collagen protein "collagen alpha-2(I) chain isoform X2" (accession number XP_026771581). (e) Sequence logo representation of peptide cleavage patterns. The sequence logo representation of collagen cleavage sites was visualized by implementing the ggseqlogo package in R, which is freely available at the Github repository. MW, molecular weight; p*I*, isoelectric point.

(>10 kDa) and LMW (<10 kDa) collagen hydrolysates through stepwise ultrafiltration. Size-exclusion chromatography and LC-MS/MS analysis validated the successful fractionation of collagen hydrolysates according to their molecular weights (Figure 2c and Figures S5 and S6). Most peptides were derived from collagen, whereas *L. plantarum* and *L. salivarius* collagen hydrolysates contained minor microbial peptides (Figure 3a). The three collagen hydrolysates contained distinct peptide sequences. More than 85% of the peptides were species-specific, indicating that different CPs can be produced from anaerobic digestion of collagen in a probiotics-dependent manner (Figure 3b). Interestingly, collagen hydrolysates of *L. plantarum* and *L. salivarius* shared more peptides than those of *L. paracasei*. In addition, the three hydrolysates contained peptides with similar p*I*, while their molecular weights were distributed differently (Figure 3c). The average molecular weight of collagen hydrolysates produced by *L. plantarum* was lower than that of collagen hydrolysates produced by *L. paracasei*. In contrast, peptides in the collagen hydrolysates of *L. salivarius* were spread over a wide range of molecular weights. Such distinguishing patterns in peptide sequences and their physicochemical properties revealed the diversity of peptide profiles produced during anaerobic digestion by these three species.

Peptide portfolios produced by Lactobacillaceae species imply a diversity of proteolytic systems and the expansion of peptide availability. Mapping of CPs onto a representative collagen protein, "collagen alpha-2(I) chain isoform X2" (accession number XP_026771581) indicated that the distribution of peptides from each hydrolysate is complementary to one another in cleaving the collagen proteins (Figure 3d). Moreover, the cleavage patterns of bacterial proteases were inferred by analyzing the residues in the C-terminal and N-

https://doi.org/10.1021/acs.jafc.2c01251
J. Agric. Food Chem. 2022, 70, 8365−8376

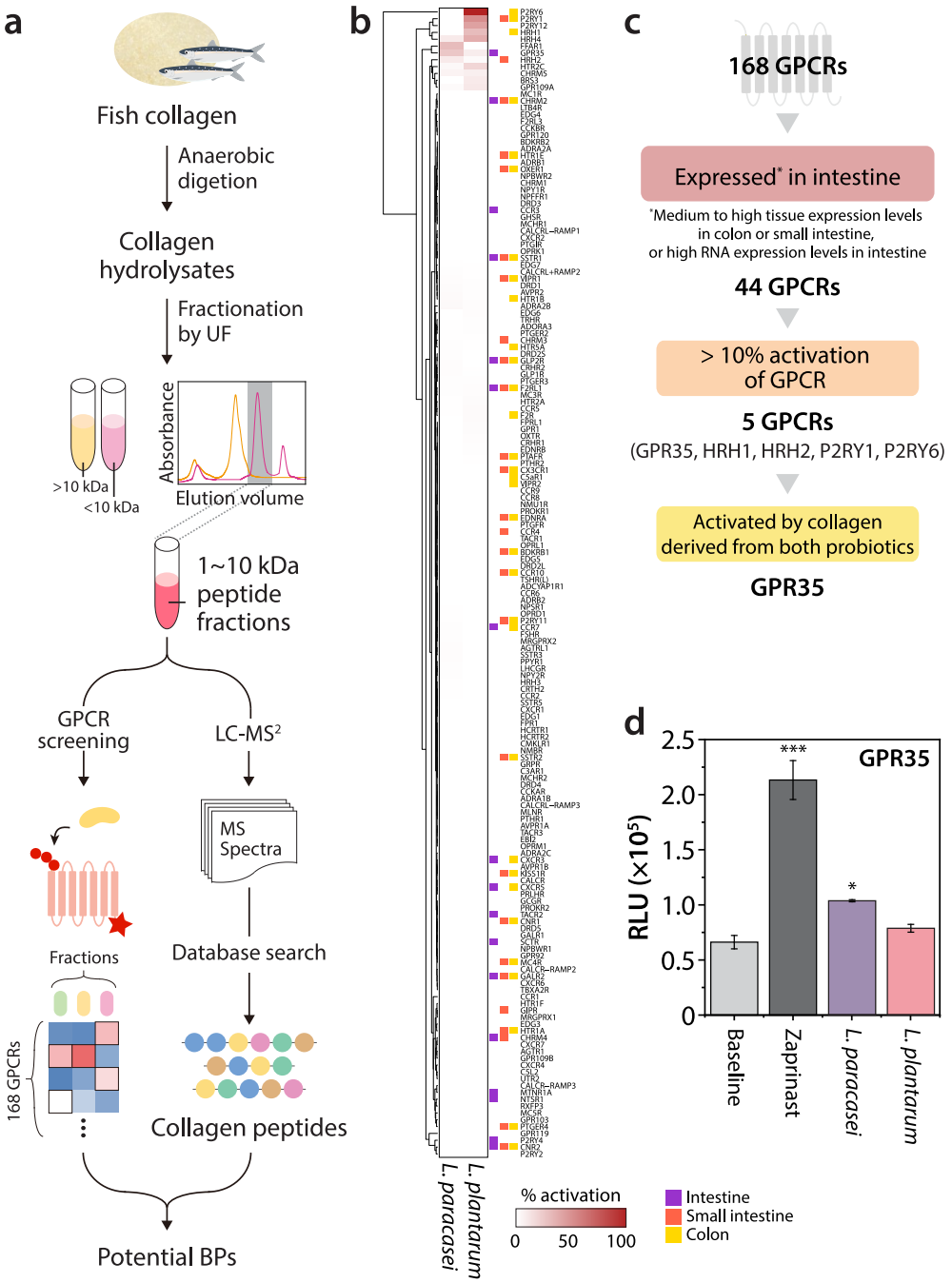

Figure 4. Collagen peptides (CPs) as potential GPR35 agonistic ligands. (a) Experimental scheme to identify potential bioactive peptides from collagen hydrolysates based on functional screening and peptide identification. (b) Heatmap of individual agonist assays for 168 G protein-coupled receptors (GPCRs). Activities were measured using β-arrestin recruitment, with each measurement normalized to control agonists (100%). GPCRs were labeled for their expression (tissue or RNA) in the small intestine and colon. (c) Screening procedure to identify potential GPCRs with CP as agonistic ligand. (d) Activation of GPR35 by *L. paracasei* and *L. plantarum* CPs, measured in terms of relative light unit (RLU). GPCR, G protein-coupled receptor; RLU, relative light unit; UF, ultrafiltration.

terminal directions. More than 70% of peptides generated by *L. paracasei* presented glycine (G) at the P1′ and P3 sites (Figure 3e). In contrast, aspartate (D) and glycine (G), as well as glycine (G) and proline (P), were found at the P1 and P1′ sites, respectively, for *L. plantarum* and *L. salivarius*. Collectively, *L. paracasei* and *L. plantarum* (or *L. salivarius*) produce unique peptide profiles, presumably due to different protease/peptidase repertoires. On the other hand, *L. plantarum* and *L. salivarius* seemingly share more in common with respect to their cleavage patterns.

Screening of CPs Showing Agonistic Activities for GPCRs in the Human Gut. Of the three species, *L. plantarum* and *L. paracasei* were selected for functional screening using β-arrestin recruitment assays for GPCRs because *L. salivarius* showed very similar protein cleavage patterns as *L. plantarum* (Figure 3e). Collagen hydrolysates from both strains were subjected to further purification to obtain 1−10 kDa peptide fractions (Figures 2c and 4a). To determine the optimal concentrations for cell-based functional screening, we tested the cytotoxicity of the peptide fractions in Caco-2 cells. CP fractions

https://doi.org/10.1021/acs.jafc.2c01251
J. Agric. Food Chem. 2022, 70, 8365−8376

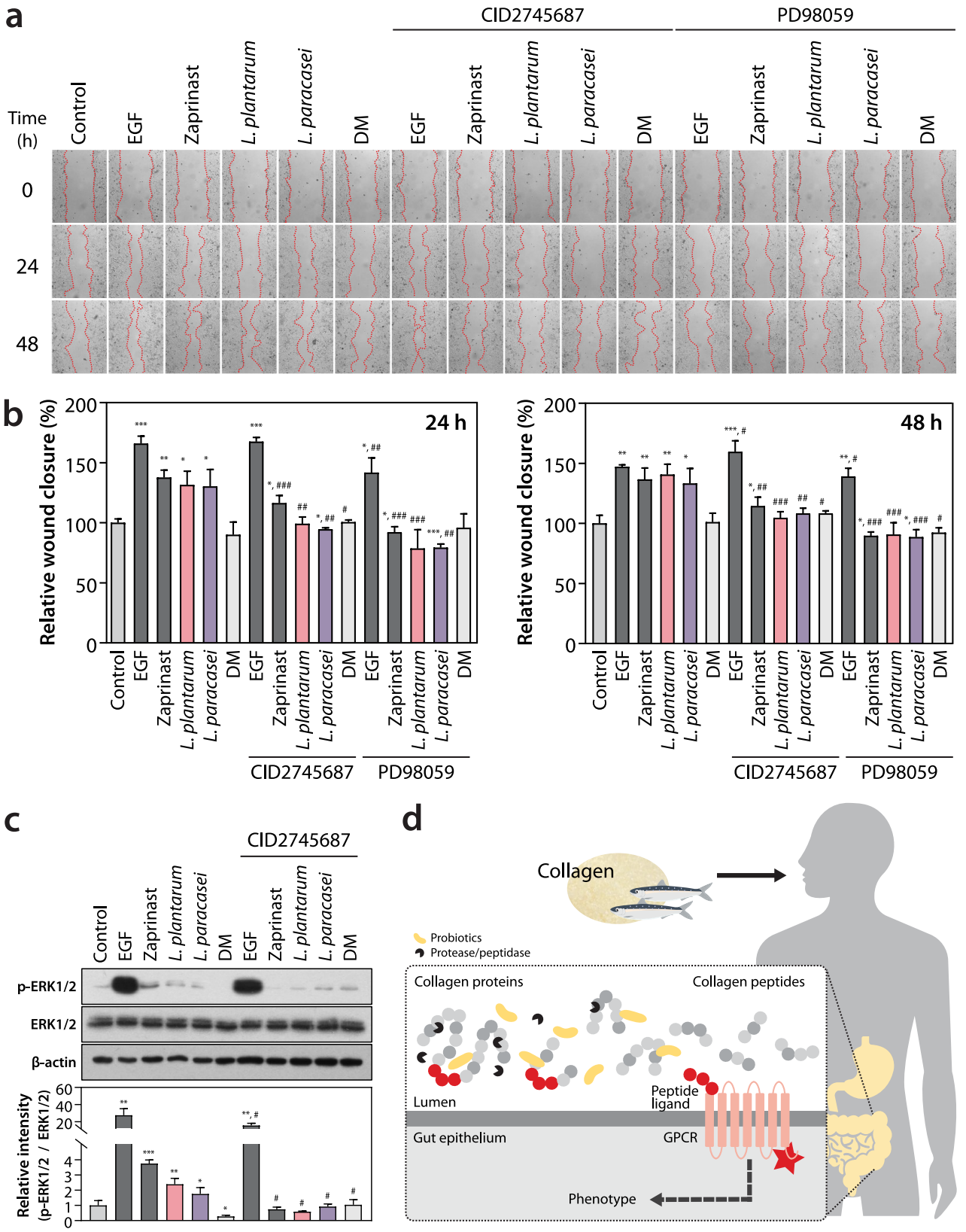

Figure 5. GPR35-induced wound healing effects of collagen peptides (CPs). (a) Wound healing effects of *L. plantarum* and *L. paracasei* CP fractions in Caco-2 cells. Cells were preincubated in serum-free EMEM with or without specific antagonists (CID 2745687 at 0.1 μM or PD98059 at 10 μM) for 1 h before scratching. After scratching, the cells were further treated with CP fractions (20 μg/mL), equal fractions of DMC (20 μg/mL), positive controls (20 ng/mL EGF or 2 μM zaprinast), or a vehicle for 48 h. The wound width of Caco-2 cells was visualized at intervals of 24 h. Scale bar, 200 μm. (b) Relative wound closure rates (%) in part a. (c) Effects of the CP fractions on ERK1/2 signaling pathway in Caco-2 cells. The starved cells were pretreated with or without CID 2745687 (0.1 μM) for 1 h and incubated for 5 min in the presence or absence of CP fractions (20 μg/mL), equal fractions of DMC (20 μg/mL), or positive controls (20 ng/mL EGF or 2 μM zaprinast). Western blot analyses were performed to evaluate

https://doi.org/10.1021/acs.jafc.2c01251
J. Agric. Food Chem. 2022, 70, 8365−8376

Figure 5. continued

phosphorylation of ERK1/2. Statistical differences were examined using unpaired student's *t*-test. ***$p < 0.001$, **$p < 0.01$, and *$p < 0.05$, compared to the untreated control; ###$p < 0.001$, ##$p < 0.01$, and #$p < 0.05$, compared to each test group treated without inhibitors. Values are represented as mean ± SD ($n = 3$). The data shown are representative of experiments performed independently three times. (d) Schematic diagram of fish collagen digestion in the human gut. Collagen goes down the digestive system and reaches the intestine, where bacterial proteases (black) digest proteins to produce CPs (gray and red circles depicting amino acids). Bioactive peptide (red circles) binds to the gut epithelial receptors and activates the downstream signaling pathway. DM, defined media; EGF, epidermal growth factor; ERK, extracellular signal-regulated kinase; GPCR, G protein-coupled receptor.

at concentrations up to 1 mg/mL retained 80% viability in Caco-2 cells after treatment for up to 48 h (Figure S7).

We examined the agonistic activity of the peptide fractions of 168 GPCRs (Figure 4b). Overall, collagen hydrolysates produced by *L. plantarum* highly activated (>20% agonistic activity) purinergic GPCRs (P2RY1, P2RY6, and P2RY12) and histamine receptors (HRH1 and HRH4). Collagen hydrolysates produced by *L. paracasei* highly activated FFAR1 and GPR35 receptors while moderately activating (>10%) HRH receptors. Of all the GPCRs screened, 44 GPCRs showed medium to high tissue expression or high RNA expression in the human gut. In particular, five GPCRs (GPR35, HRH1, HRH2, P2RY1, and P2RY6) were noticeably activated by >10%, as compared to the control agonist activities (Figure 4c). Remarkably, GPR35, a class A rhodopsin-like GPCR, was activated by CPs from both probiotics. GPR35 contributes to intestinal homeostasis with respect to colitis, bacterial infections, and colorectal cancers.[23] The 1−10 kDa peptide fractions of *L. paracasei* and *L. plantarum* were 25.5% and 8.6% activated, respectively, compared to zaprinast, a well-known agonist (Figure 4d). These results highlight the potential of CPs produced by *L. paracasei* and *L. plantarum* in promoting gut health by communicating with host cells via GPCRs.

Wound Healing Assay of CPs Using Colonocytes. Based on their phenotypes in the intestinal epithelium, we examined the ability of the *L. plantarum* and *L. paracasei* CP fractions to serve as GPCR agonists. To investigate their wound healing capabilities, we treated scratched Caco-2 cells, which are human colon epithelial cells, with each CP fraction. EGF, a well-known wound healing agent, and zaprinast, an agonist of GPR35, were used as positive controls. *L. plantarum* and *L. paracasei* peptide fractions significantly promoted wound closure in Caco-2 cells, as compared to the control (Figure 5a,b). To verify GPR35-mediated wound healing activities, we preincubated cells with CID 2745687 and PD98059 to inhibit GPR35 and ERK1/2 signaling pathway, respectively. Inhibition of GPR35 abolished the wound healing activities of the peptide fractions and zaprinast but failed to reverse the effect of EGF (Figure 5a,b). Remarkably, *L. plantarum* and *L. paracasei* CP fractions showed wound closure activities comparable to those of zaprinast. Despite relatively marginal GPR35-binding activities (Figure 4d), CP fractions from both strains exhibited pronounced wound healing activities (Figure 5a,b), which might be ascribed to other receptors and/or signaling pathways involved in intestinal epithelial cells.[24,25] Further, zaprinast, *L. plantarum*, and *L. paracasei* CP fractions increased ERK1/2 phosphorylation in Caco-2 cells by 3.76 ± 0.2-fold, 2.39 ± 0.4-fold, and 1.76 ± 0.41-fold, respectively (Figure 5c). Such effects were reversed upon treatment with CID 2745687, which down-regulated the ERK1/2 signaling pathway by inhibiting GPR35. Taken together, these results indicated that *L. plantarum* and *L. paracasei* CP fractions promote wound healing through the GPR35-mediated ERK1/2 signaling pathway in Caco-2 cells.

DISCUSSION

Excavation of beneficial BPs from appropriate food sources requires an integrated approach to predict the potential health benefits of dietary sources and screen proteolytic systems in the gut microbiota. In the present study, we designed and developed a genomics-aided semirational strategy to screen Lactobacillaceae species as potential biocatalysts to produce bioactive CPs. Unlike conventional top-down approaches for designing and screening thousands of peptides for a diverse array of functions,[6,26] we sought to choose appropriate biocatalysts by profiling the repertoires of proteases in Lactobacillaceae using genome and protease data.

Beyond the physiological effects of chemical constituents in food, the importance of dietary intake derives from the way it shapes the intestinal microbiota.[27] In the human GI tract, gut microbiota releases food-derived bioactive compounds, including BPs, that human enzymes cannot produce, which act as primary stimulus and regulate diverse host immune cells.[14] Although the underlying mechanisms are not fully understood, they are likely to be mediated by changes in the intestinal microbiota and their metabolic products. Fish and its constituents (e.g., omega-3 fatty acids, melatonin, collagen, etc.) present biological properties that favorably modulate immune functions. In particular, a lean-seafood diet, compared to a nonseafood protein diet, reduces the risk of cardiovascular disease by modulating the gut microbiota and the metabolites generated.[28,29] In this regard, we conducted *in silico* digestion, as described previously, to screen for novel BPs encrypted in fish collagen sequences.[6] Our genome-aided *in silico* proteolytic analysis indicated that bacterial proteases could create differential profiles of specific BPs released from collagen that differ from those of BPs generated by mammalian proteases. This result underlines the importance of gut microbial proteases as complementary biocatalysts in the human GI tract (Figure 1a). In particular, BPs exert diverse physiological functions as cellular signaling molecules for various cell surface receptors, such as GPCRs and toll-like receptors.[30]

LAB, a resident flora of the gut, has been recognized as a safe and health-promoting bacterium because it can produce a variety of bioactive compounds in fermented foods or human gut microbiota in the GI tract.[21,31] In addition to the conventional probiotic effect of LAB on human health, recent scientific evidence supports the notion that LAB can transform food proteins into BPs and biogenic amines using proteolytic enzymes.[32] The possession of various proteases evolved presumably due to their amino acid auxotrophy, which makes Lactobacillaceae species potential BP producers; their proteolytic activity places these bacteria as beneficial probiotics that can transform dietary components into health-promoting nutraceuticals in vertebrates.[33] In this regard, probiotic lactobacilli in the upper part of the GI tract continue to gain momentum as potential key players in the production of BPs from collagen as a source of animal protein.[34]

https://doi.org/10.1021/acs.jafc.2c01251
J. Agric. Food Chem. 2022, 70, 8365−8376

Genome comparison of Lactobacillaceae revealed distinct clusters even within the same family, which coincided with previous comparative genomic analyses (Figure 1b,c).[35] Interestingly, species in C3 possessed fewer serine proteases (S) and metalloproteases (M) than those in C2 and C4. On the other hand, species in C2 had the highest number of cysteine (C) peptidases. In addition, commercially valuable probiotics such as *L. casei*, *L. paracasei*, and *L. rhamnosus* in C4 were closely related.[36] Nevertheless, POCP analysis based on concatenated conserved core gene sequences and comparative protease profiles discriminated individual Lactobacillaceae at the species level that belonged to the same cluster. Such systematic analysis at the genome level enabled us to choose potential BP producers efficiently. The genome-based analysis of laboratories was further cross-validated in terms of the differential growth-enhancing effect of collagen on 10 Lactobacillaceae species (Figure 2a,b) and by analyzing collagen hydrolysis patterns in their culture supernatants (Figure 2c). Collectively, these results indicated that the metabolic functions of Lactobacillaceae species from separate clusters could have different collagen-degrading capacities.

Microbiota-specific metabolites such as SCFAs and BPs function as potent modulatory factors for human health via host−gut microbiota crosstalk.[14,15,20] For example, butyrate produced by *Faecalibacterium prausnitzii* exerts anti-inflammatory effects in intestinal epithelial cells via modulation of Dact3, a gene linked to the Wnt/JNK pathway.[37] In addition, *Lactobacillus reuteri* produces AhR agonists, thereby restoring the gut barrier defect and secretion of GLP-1.[38] According to our MS analysis of collagen hydrolysates, all three species used in this study could hydrolyze collagen proteins to produce LMW peptides. However, the peptide profiles (sequences and physicochemical properties) and protein cleavage patterns varied (Figure 3b−e). Notably, *L. paracasei* produced more distinct patterns than the other species. Such differences in cleavage patterns coincide with the comparative genomic data and differential protease repertoires of Lactobacillaceae species (Figure 1). In this regard, various probiotics can substitute their roles among other LAB, and any specific LAB exhibits unique biological activity. The CP fractions showed different binding activities toward GPCRs, in a species-specific manner. Despite the low purity of the sample, several GPCRs in the gut were moderately activated by the peptide fractions (Figure 4b). This result highlights the potential of collagen BPs to function as binding ligands for GPCRs, thereby communicating with host cells. We explored the physiological function of the agonist activity of *L. plantarum* and *L. paracasei* collagen hydrolysates against specific GPCRs in the intestinal epithelium. GPR35, a GPCR highly expressed in the GI tract in humans, was activated by CP fractions produced by both Lactobacillaceae species.[39] A recent study reported that GPR35 agonists promote wound healing by activating the EKR1/2 signaling pathway in young adult mouse colon epithelial cells, suggesting that GPR35 is involved in the maintenance of mucosal morphology and intestinal integrity.[40] Consistent with this, the present study showed that collagen hydrolysates repair wounds in human intestinal epithelial cells through GPR35-mediated ERK1/2 signaling (Figure 5). The intestinal epithelium acts as a barrier that protects the host from harmful factors in the lumen, such as toxins, antigens, and pathogens.[41] Loss of function of the intestinal epithelial barrier causes an excessive inflammatory response upon exposure of these harmful factors to the immune system, thereby leading to diseases of the GI tract, including IBD.[42] A single nucleotide polymorphism in the GPR35 gene has been shown to be correlated with the onset of disease in IBD patients.[43,44] These results suggest that *L. plantarum* and *L. paracasei* CP fractions with GPR35 agonist activity may be candidates for nutraceutical and medical food agents that can alleviate diseases related to intestinal barrier disorders such as IBD.

The genomics-aided semirational approach in the present study provided a list of putative BPs that show the potential to serve as gut probiotics capable of modulating the GI environment through hydrolysis of food proteins. Considering the demands for means of life quality improvement and disease prevention, LAB-aided BPs derived from collagen may play a crucial role in mediating host cell signaling. In particular, LAB-aided postbiotic CPs, instead of more transient empiric probiotic supplementation that encounters a marked mucosal colonization resistance,[45] may be more effective and applicable for various industrial applications, ranging from nutraceuticals to medical foods.

■ ASSOCIATED CONTENT

Supporting Information

The Supporting Information is available free of charge at https://pubs.acs.org/doi/10.1021/acs.jafc.2c01251.

Table S1, genomic features of *Lactobacillus* type strains; Table S2, defined media (DM) composition of *Lactobacillus* species; Table S3, list of collagen peptides identified from anaerobic digestion by *L. paracasei*; Table S4, list of collagen peptides identified from anaerobic digestion by *L. plantarum*; Table S5, list of collagen peptides identified from anaerobic digestion by *L. salivarius*; Figure S1, families of proteolytic enzymes in Lactobacillaceae; Figure S2, anaerobic fermentation of collagen by Lactobacillaceae species; Figure S3, SDS-PAGE analysis of culture supernatants from anaerobic fermentation of collagen by four representative Lactobacillaceae species; Figure S4, representative MS spectra of collagen peptides and fragment ions produced by *L. paracasei*, *L. plantarum*, and *L. salivarius*; Figure S5, calibration curve for Superdex 30 pg gel filtration chromatography; Figure S6, peptide length distributions in high molecular weight (HMW, >10 kDa) and low molecular weight (LMW, <10 kDa) collagen hydrolysates produced by Lactobacillaceae; and Figure S7, cytotoxicity of collagen peptide fractions in Caco-2 cells (PDF)

■ AUTHOR INFORMATION

Corresponding Author

Dong-Woo Lee − *Department of Biotechnology and Department of Bioindustrial Engineering, Yonsei University, Seoul 03722, South Korea;* orcid.org/0000-0002-2272-8321; Phone: +82-2-2123-2886; Email: leehicam@yonsei.ac.kr; Fax: +82-2-362-7265

Authors

Ji-Young Lee − *Department of Biotechnology, Yonsei University, Seoul 03722, South Korea*

Hye Won Hwang − *Department of Bioindustrial Engineering, Yonsei University, Seoul 03722, South Korea*

Hyeon-Su Jin − *Department of Biotechnology, Yonsei University, Seoul 03722, South Korea*

Jae-Eun Lee − *Department of Biotechnology, Yonsei University, Seoul 03722, South Korea*
Nam Joo Kang − *School of Food Science and Biotechnology, Kyungpook National University, Daegu 41566, South Korea*

Complete contact information is available at: https://pubs.acs.org/10.1021/acs.jafc.2c01251

Author Contributions

[¶]J.-Y.Lee and H. W. Hwang contributed equally to this work. J.-Y. Lee, H. W. Hwang, H.-S. Jin, J.-E. Lee, N. J. Kang, and D.-W. Lee formulated the research plan. J.-Y. Lee, H. W. Hwang, H.-S. Jin, and J.-E. Lee performed the experiments. J.-Y. Lee, H. W. Hwang, J.-E. Lee, H.-S. Jin, N. J. Kang, and D.-W. Lee analyzed the data. J.-Y. Lee, H. W. Hwang, J.-E. Lee, and D.-W. Lee wrote the manuscript. N. J. Kang and D.-W. Lee conceived, planned, supervised, and managed the study.

Funding

This work was supported by a grant from the Korea Health Technology R&D Project through the Korea Health Industry Development Institute (KHIDI), funded by the Ministry of Health & Welfare, Republic of Korea (Grant Number HP20C0082) and the National Research Foundation of Korea (NRF) grant (Grant Number 2021M3A9I4021431), funded by the Ministry of Science, ICT, and Future Planning.

Notes

The authors declare no competing financial interest.

■ ACKNOWLEDGMENTS

We thank the staff at Newtree Co., Ltd. (Republic of Korea) for providing the fish gelatin.

■ ABBREVIATIONS USED

BP, bioactive peptide; CP, collagen peptide; DM, defined media; EMEM, Eagle's minimum essential medium; EGF, human epidermal growth factor; FA, formic acid; GI, gastrointestinal; GPCR, G-protein-coupled receptor; HMW, high molecular weight; IBD, inflammatory bowel disease; p*I*, isoelectric point; KCCM, Korean Culture Center of Microorganisms; LMW, low molecular weight; MTT, thiazolyl blue tetrazolium bromide; NCBI, National Center for Biotechnological Information; POCP, percentage of conserved proteins

■ REFERENCES

(1) Buchwald, H.; Dorman, R. B.; Rasmus, N. F.; Michalek, V. N.; Landvik, N. M.; Ikramuddin, S. Effects on GLP-1, PYY, and leptin by direct stimulation of terminal ileum and cecum in humans: implications for ileal transposition. *Surg. Obes. Relat. Dis.* **2014**, *10* (5), 780−786.
(2) Muttenthaler, M.; King, G. F.; Adams, D. J.; Alewood, P. F. Trends in peptide drug discovery. *Nat. Rev. Drug Discovery* **2021**, *20* (4), 309−325.
(3) Jin, H. S.; Song, K. S.; Baek, J. H.; Lee, J. E.; Kim, D. J.; Nam, G. W.; Kang, N. J.; Lee, D. W. Identification of matrix metalloproteinase-1-suppressive peptides in feather keratin hydrolysate. *J. Agric. Food Chem.* **2018**, *66* (48), 12719−12729.
(4) Fosgerau, K.; Hoffmann, T. Peptide therapeutics: current status and future directions. *Drug Discovery Today* **2015**, *20* (1), 122−128.
(5) Giacometti, J.; Buretić-Tomljanović, A. Peptidomics as a tool for characterizing bioactive milk peptides. *Food Chem.* **2017**, *230*, 91−98.
(6) Kang, N. J.; Jin, H. S.; Lee, S. E.; Kim, H. J.; Koh, H.; Lee, D. W. New approaches towards the discovery and evaluation of bioactive peptides from natural resources. *Crit. Rev. Environ. Sci. Technol.* **2020**, *50* (1), 72−103.
(7) Ngo, D.; Vo, T.; Ngo, D.; Wijesekara, I.; Kim, S. Biological activities and potential health benefits of bioactive peptides derived from marine organisms. *Int. J. Biol. Macromol.* **2012**, *51* (4), 378−383.
(8) Nuñez, S. M.; Guzmán, F.; Valencia, P.; Almonacid, S.; Cárdenas, C. Collagen as a source of bioactive peptides: a bioinformatics approach. *Electron. J. Biotechn.* **2020**, *48*, 101−108.
(9) Gómez-Guillén, M. C.; Giménez, B.; López-Caballero, M. E.; Montero, M. P. Functional and bioactive properties of collagen and gelatin from alternative sources: a review. *Food Hydrocolloid.* **2011**, *25* (8), 1813−1827.
(10) Mei, F.; Liu, J.; Wu, J.; Duan, Z.; Chen, M.; Meng, K.; Chen, S.; Shen, X.; Xia, G.; Zhao, M. Collagen peptides isolated from *Salmo salar* and *Tilapia nilotica* skin accelerate wound healing by altering cutaneous microbiome colonization via upregulated NOD2 and BD14. *J. Agric. Food Chem.* **2020**, *68* (6), 1621−1633.
(11) Zdzieblik, D.; Oesser, S.; Baumstark, M. W.; Gollhofer, A.; König, D. Collagen peptide supplementation in combination with resistance training improves body composition and increases muscle strength in elderly sarcopenic men: a randomised controlled trial. *Br. J. Nutr.* **2015**, *114* (8), 1237−1245.
(12) Lee, E. J.; Hur, J.; Ham, S. A.; Jo, Y.; Lee, S.; Choi, M.-J.; Seo, H. G. Fish collagen peptide inhibits the adipogenic differentiation of preadipocytes and ameliorates obesity in high fat diet-fed mice. *Int. J. Biol. Macromol.* **2017**, *104*, 281−286.
(13) Tang, Z.; Chen, G.; Hong, Q.; Huang, S.; Smith, H. M.; Shah, R. D.; Scholz, M.; Ferguson, J. F. Multi-omic analysis of the microbiome and metabolome in healthy subjects reveals microbiome-dependent relationships between diet and metabolites. *Front. Genet.* **2019**, *10*, 454.
(14) Kelly, C. J.; Zheng, L.; Campbell, E. L.; Saeedi, B.; Scholz, C. C.; Bayless, A. J.; Wilson, K. E.; Glover, L. E.; Kominsky, D. J.; Magnuson, A.; Weir, T. L.; Ehrentraut, S. F.; Pickel, C.; Kuhn, K. A.; Lanis, J. M.; Nguyen, V.; Taylor, C. T.; Colgan, S. P. Crosstalk between microbiota-derived short-chain fatty acids and intestinal epithelial HIF augments tissue barrier function. *Cell Host & Microbe.* **2015**, *17* (5), 662−671.
(15) Fan, Y.; Pedersen, O. Gut microbiota in human metabolic health and disease. *Nat. Rev. Microbiol.* **2021**, *19* (1), 55−71.
(16) Young, D.; Ibuki, M.; Nakamori, T.; Fan, M.; Mine, Y. Soy-derived di- and tripeptides alleviate colon and ileum inflammation in pigs with dextran sodium sulfate-induced colitis. *J. Nutr.* **2012**, *142* (2), 363−368.
(17) Cohen, L. J.; Esterhazy, D.; Kim, S.-H.; Lemetre, C.; Aguilar, R. R.; Gordon, E. A.; Pickard, A. J.; Cross, J. R.; Emiliano, A. B.; Han, S. M.; Chu, J.; Vila-Farres, X.; Kaplitt, J.; Rogoz, A.; Calle, P. Y.; Hunter, C.; Bitok, J. K.; Brady, S. F. Commensal bacteria make GPCR ligands that mimic human signalling molecules. *Nature* **2017**, *549* (7670), 48−53.
(18) The Integrative HMP (iHMP) Research Network Consortium. The Integrative Human Microbiome Project. *Nature* **2019**, *569* (7758), 641−648.
(19) Griffiths, M. W.; Tellez, A. M. *Lactobacillus helveticus*: the proteolytic system. *Front. Microbiol.* **2013**, *4*, 30.
(20) Pasolli, E.; De Filippis, F.; Mauriello, I. E.; Cumbo, F.; Walsh, A. M.; Leech, J.; Cotter, P. D.; Segata, N.; Ercolini, D. Large-scale genome-wide analysis links lactic acid bacteria from food with the gut microbiome. *Nat. Commun.* **2020**, *11*, 2610.
(21) Tannock, G. W. A special fondness for *Lactobacilli*. *Appl. Environ. Microbiol.* **2004**, *70* (6), 3189−3194.
(22) Saguir, F. M.; de Nadra, M. C. M. Improvement of a chemically defined medium for the sustained growth of *Lactobacillus plantarum*: nutritional requirements. *Curr. Microbiol.* **2007**, *54* (6), 414.
(23) Kaya, B.; Melhem, H.; Niess, J. H. GPR35 in intestinal diseases: from risk gene to function. *Front. Immunol.* **2021**, *12*, 717392.
(24) Fernando, E. H.; Gordon, M. H.; Beck, P. L.; MacNaughton, W. K. Inhibition of intestinal epithelial wound healing through protease-activated receptor-2 activation in Caco2 cells. *J. Pharmacol. Exp. Ther.* **2018**, *367* (2), 382−392.
(25) Iizuka, M.; Konno, S. Wound healing of intestinal epithelial cells. *World J. Gastroentero.* **2011**, *17* (17), 2161−2171.
(26) Hayes, M.; Stanton, C.; Fitzgerald, G. F.; Ross, R. P. Putting microbes to work: dairy fermentation, cell factories and bioactive

peptides. Part II: bioactive peptide functions. *Biotechnol. J.* **2007**, *2* (4), 435−449.
(27) Mendivil, C. O. Dietary fish, fish nutrients, and immune function: a review. *Front. Nutr.* **2021**, *7*, 617652.
(28) Aadland, E. K.; Lavigne, C.; Graff, I. E.; Eng, Ø.; Paquette, M.; Holthe, A.; Mellgren, G.; Jacques, H.; Liaset, B. Lean-seafood intake reduces cardiovascular lipid risk factors in healthy subjects: results from a randomized controlled trial with a crossover design. *Am. J. Clin. Nutr.* **2015**, *102* (3), 582−592.
(29) Schmedes, M.; Brejnrod, A. D.; Aadland, E. K.; Kiilerich, P.; Kristiansen, K.; Jacques, H.; Lavigne, C.; Graff, I. E.; Eng, Ø.; Holthe, A.; Mellgren, G.; Young, J. F.; Sundekilde, U. K.; Liaset, B.; Bertram, H. C. The effect of lean-seafood and non-seafood diets on fecal metabolites and gut microbiome: results from a randomized crossover intervention study. *Mol. Nutr. Food Res.* **2019**, *63* (1), 1700976.
(30) Muratspahic, E.; Freissmuth, M.; Gruber, C. W. Nature-derived Peptides: a growing niche for GPCR ligand discovery. *Trends Pharmacol. Sci.* **2019**, *40* (5), 309−326.
(31) Gilliland, S. E. Health and nutritional benefits from lactic acid bacteria. *FEMS Microbiol. Rev.* **1990**, *7* (1−2), 175−188.
(32) Pessione, E.; Cirrincione, S. Bioactive molecules released in food by lactic acid bacteria: encrypted peptides and biogenic amines. *Front. Microbiol.* **2016**, *7*, 876.
(33) Raveschot, C.; Cudennec, B.; Coutte, F.; Flahaut, C.; Fremont, M.; Drider, D.; Dhulster, P. Production of bioactive peptides by *Lactobacillus* species: from gene to application. *Front. Microbiol.* **2018**, *9*, 2354.
(34) Sandine, W. E. Roles of *Lactobacillus* in the intestinal tract. *J. Food Prot.* **1979**, *42* (3), 259−262.
(35) Sun, Z.; Harris, H. M. B.; McCann, A.; Guo, C.; Argimón, S.; Zhang, W.; Yang, X.; Jeffery, I. B.; Cooney, J. C.; Kagawa, T. F.; Liu, W.; Song, Y.; Salvetti, E.; Wrobel, A.; Rasinkangas, P.; Parkhill, J.; Rea, M. C.; O'Sullivan, O.; Ritari, J.; Douillard, F. P.; Paul Ross, R.; Yang, R.; Briner, A. E.; Felis, G. E.; de Vos, W. M.; Barrangou, R.; Klaenhammer, T. R.; Caufield, P. W.; Cui, Y.; Zhang, H.; O'Toole, P. W. Expanding the biotechnology potential of *Lactobacilli* through comparative genomics of 213 strains and associated genera. *Nat. Commun.* **2015**, *6* (1), 8322.
(36) Huang, C.; Li, S.; Huang, L.; Watanabe, K. Identification and classification for the *Lactobacillus casei* group. *Front. Microbiol.* **2018**, *9*, 1974.
(37) Lenoir, M.; Martín, R.; Torres-Maravilla, E.; Chadi, S.; González-Dávila, P.; Sokol, H.; Langella, P.; Chain, F.; Bermúdez-Humarán, L. G. Butyrate mediates anti-inflammatory effects of *Faecalibacterium prausnitzii* in intestinal epithelial cells through *Dact3*. *Gut Microbes* **2020**, *12* (1), 1826748.
(38) Natividad, J. M.; Agus, A.; Planchais, J.; Lamas, B.; Jarry, A. C.; Martin, R.; Michel, M.-L.; Chong-Nguyen, C.; Roussel, R.; Straube, M.; Jegou, S.; McQuitty, C.; Le Gall, M.; da Costa, G.; Lecornet, E.; Michaudel, C.; Modoux, M.; Glodt, J.; Bridonneau, C.; Sovran, B.; Dupraz, L.; Bado, A.; Richard, M. L.; Langella, P.; Hansel, B.; Launay, J.-M.; Xavier, R. J.; Duboc, H.; Sokol, H. Impaired aryl hydrocarbon receptor ligand production by the gut microbiota is a key factor in metabolic syndrome. *Cell Metab.* **2018**, *28* (5), 737−749.
(39) McCallum, J. E.; Mackenzie, A. E.; Divorty, N.; Clarke, C.; Delles, C.; Milligan, G.; Nicklin, S. A. G-protein-coupled Receptor 35 mediates human saphenous vein vascular smooth muscle cell migration and endothelial cell proliferation. *J. Vasc. Res.* **2016**, *52* (6), 383−95.
(40) Tsukahara, T.; Hamouda, N.; Utsumi, D.; Matsumoto, K.; Amagase, K.; Kato, S. G protein-coupled receptor 35 contributes to mucosal repair in mice via migration of colonic epithelial cells. *Pharmacol. Res.* **2017**, *123*, 27−39.
(41) Allaire, J. M.; Crowley, S. M.; Law, H. T.; Chang, S. Y.; Ko, H. J.; Vallance, B. A. The intestinal epithelium: central coordinator of mucosal immunity. *Trends Immunol.* **2018**, *39* (9), 677−696.
(42) Roda, G.; Sartini, A.; Zambon, E.; Calafiore, A.; Marocchi, M.; Caponi, A.; Belluzzi, A.; Roda, E. Intestinal epithelial cells in inflammatory bowel diseases. *World J. Gastroentero.* **2010**, *16* (34), 4264−4271.
(43) Ellinghaus, D.; Folseraas, T.; Holm, K.; Ellinghaus, E.; Melum, E.; Balschun, T.; Laerdahl, J. K.; Shiryaev, A.; Gotthardt, D. N.; Weismuller, T. J.; Schramm, C.; Wittig, M.; Bergquist, A.; Bjornsson, E.; Marschall, H. U.; Vatn, M.; Teufel, A.; Rust, C.; Gieger, C.; Wichmann, H. E.; Runz, H.; Sterneck, M.; Rupp, C.; Braun, F.; Weersma, R. K.; Wijmenga, C.; Ponsioen, C. Y.; Mathew, C. G.; Rutgeerts, P.; Vermeire, S.; Schrumpf, E.; Hov, J. R.; Manns, M. P.; Boberg, K. M.; Schreiber, S.; Franke, A.; Karlsen, T. H. Genome-wide association analysis in primary sclerosing cholangitis and ulcerative colitis identifies risk loci at GPR35 and TCF4. *Hepatology* **2013**, *58* (3), 1074−1083.
(44) Yang, S. K.; Hong, M.; Choi, H.; Zhao, W.; Jung, Y.; Haritunians, T.; Ye, B. D.; Kim, K. J.; Park, S. H.; Lee, I.; Kim, W. H.; Cheon, J. H.; Kim, Y. H.; Jang, B. I.; Kim, H. S.; Choi, J. H.; Koo, J. S.; Lee, J. H.; Jung, S. A.; Shin, H. D.; Kang, D.; Youn, H. S.; Taylor, K. D.; Rotter, J. I.; Liu, J.; McGovern, D. P.; Song, K. Immunochip analysis identification of 6 additional susceptibility loci for Crohn's disease in Koreans. *Inflamm. Bowel. Dis.* **2015**, *21* (1), 1−7.
(45) Zmora, N.; Zilberman-Schapira, G.; Suez, J.; Mor, U.; Dori-Bachash, M.; Bashiardes, S.; Kotler, E.; Zur, M.; Regev-Lehavi, D.; Brik, R. B.; Federici, S.; Cohen, Y.; Linevsky, R.; Rothschild, D.; Moor, A. E.; Ben-Moshe, S.; Harmelin, A.; Itzkovitz, S.; Maharshak, N.; Shibolet, O.; Shapiro, H.; Pevsner-Fischer, M.; Sharon, I.; Halpern, Z.; Segal, E.; Elinav, E. Personalized gut mucosal colonization resistance to empiric probiotics is associated with unique host and microbiome features. *Cell* **2018**, *174* (6), 1388−1405.

https://doi.org/10.1021/acs.jafc.2c01251
J. Agric. Food Chem. 2022, 70, 8365−8376